

AnchorFormer: Differentiable Anchor Attention for Efficient Vision Transformer

Jiquan Shan¹, Junxiao Wang¹, Lifeng Zhao¹, Liang Cai¹, Hongyuan Zhang², Ioannis Lirantzis^{3,4*}

¹PetroChina Changqing Oilfield Company, Xi'an, Shaanxi, China

²The University of Hong Kong

³Alma Mater Europaea University

⁴South China University of Technology, Guangzhou, Guangdong, China

Abstract

Recently, vision transformers (ViTs) have achieved excellent performance on vision tasks by measuring the global self-attention among the image patches. Given n patches, they will have quadratic complexity such as $\mathcal{O}(n^2)$ and the time cost is high when splitting the input image with a small granularity. Meanwhile, the pivotal information is often randomly gathered in a few regions of an input image, some tokens may not be helpful for the downstream tasks. To handle this problem, we introduce an anchor-based efficient vision transformer (**AnchorFormer**), which employs the anchor tokens to learn the pivotal information and accelerate the inference. Firstly, by estimating the bipartite attention between the anchors and tokens, the complexity will be reduced from $\mathcal{O}(n^2)$ to $\mathcal{O}(mn)$, where m is an anchor number and $m < n$. Notably, by representing the anchors with the neurons in a neural layer, we can differentiable learn these distributions and approximate global self-attention through the Markov process. Moreover, we extend the proposed model to three downstream tasks including classification, detection, and segmentation. Extensive experiments show the effectiveness of our AnchorFormer, e.g., achieving up to a **9.0%** higher accuracy or **46.7%** FLOPs reduction on ImageNet classification, **81.3%** higher mAP on COCO detection under comparable FLOPs, as compared to the current baselines.

1. Introduction

The powerful performance of the Transformers in the natural language processing field [49] has triggered extensive research on Transformers in the computer vision field. As core variants, vision transformers (ViTs) utilize the multi-head self-attention to extract the deep feature representation by partitioning the input images into some patches with

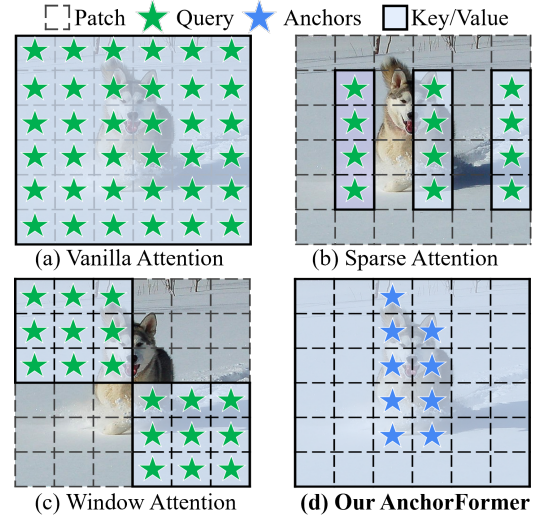


Figure 1. Comparison of the proposed and other efficient attention strategies. Fig. 1a is the vanilla self-attention in ViTs. Fig. 1b is the sparse-based attention which mainly preserves the specific queries, keys, and values. Fig. 1c is the window attention which calculates the local attention within the windows. Fig. 1d is the proposed model which focuses on highly informative regions and differentiable learning the pivotal attention.

identical granularity and processing them as sequences by positional embedding [11]. Meanwhile, thanks to capturing the global similarities among the patches, ViTs have achieved excellent performance on various vision tasks, e.g., image classification, object detection, semantic segmentation, and ancient text analysis [4, 23, 29, 33, 45, 50]. The vision transformer is also extended to multi-modal data [37]. For example, the method proposed by [26] is a very interesting and promising framework that learns the underlying relevance among various modalities by a low-dimensional manifold learning mechanism. It can effectively deal with the weak features of some modalities that

*Corresponding author.

contain a lot of noise.

While ViTs have shown effectiveness on computer vision tasks, the computation complexity is a main bottleneck to limit development. Specifically, due to estimating the global self-attention by calculating the inner product between each token, the complexity of attention grows quadratically with the number of input tokens such as $\mathcal{O}(n^2)$ [34]. It leads to excessive computation costs when handling the high-resolution inputs and will be impractical to extend on the limited memory device. To overcome this problem, a promising insight is to introduce sparse attention to ViTs [70]. It mainly limits ViTs to focus on smaller regions, not global input. Among them, PVT [52] introduces sparse attention to select and estimate the similarities among small regions by calculating the inner production among these queries and keys. Then, it will share these sparse similarities to each query-key pair and obtain global attention. However, since the informative features are distributed randomly in the input images, the sparse based methods are weak in learning the local features and even discard the informative features. Different from these sparse strategies, some researchers introduce the window attention paradigm to reduce the complexity [10, 29]. As shown in Fig. 1, they divide the input tokens into the pre-designed windows paradigm and limit the ViTs calculating the attention and extracting the deep feature within these windows. Nevertheless, window attention will introduce an extra obstacle as cross-window communication. Besides, this window paradigm also restricts the setting of the model structures like how to window shifts.

Instead of the two referred efficient strategies, a natural and effective insight is introducing the anchor tokens to represent the informative regions and learn the global self-attention based on the link between anchors and other tokens. This similar idea has been widely adopted in many fields [39, 64, 67]. Among them, [64] transmits the graph into a bipartite graph by introducing the anchors, which effectively accelerates the inference of the graph neural networks. [39] reduces the computation cost by estimating the IoU between objects and anchors. Although an anchor-based strategy can accelerate the model inference, the key concerns for extending it on ViTs are how to select the proper anchors and learn the global similarities from the anchor distributions.

In this paper, we propose an anchor-based efficient vision transformer (**AnchorFormer**) which introduces the anchor tokens to accelerate the ViTs and reduce the complexity from $\mathcal{O}(n^2)$ to $\mathcal{O}(mn)$, where m is an anchor number and $m < n$. Compared with the sparse-based method PVT, the proposed AnchorFormer can differentiable learn the pivotal information among the image datasets. Meanwhile, by the Markov process, the proposed anchor-based strategy can accurately learn the global self-attention from

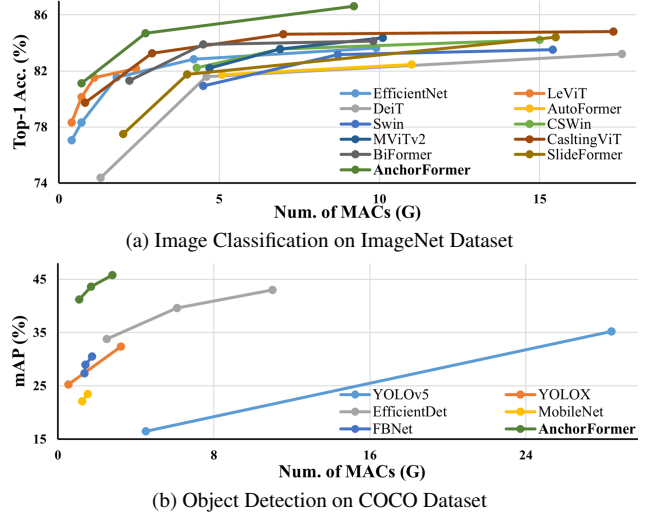


Figure 2. The proposed AnchorFormer and all baselines (EfficientNet [46], LeViT [15], DeiT [48], AutoFormer [5], Swin [29], CSWin [10], MViTv2 [27], PVT [52], CastlingViT [61], BiFormer [70], and SlideFormer [34]). Fig. 2a is the image classification results on the ImageNet dataset. Fig. 2b is the object detection results on the COCO dataset.

the anchors. Thus, it is flexible to generalize on many ViTs compared with window-based models such as Swin [29]. As shown in Fig. 2, the proposed AnchorFormer has consistently achieved the best trade-off between accuracy and efficiency over the other baselines on image classification and detection tasks. Our core contributions are as follows:

- To reduce the complexity and accelerate the ViTs, we design an anchor-based method to represent the informative queries. It can generate pivotal attention by estimating the bipartite attention between them and tokens.
- To differentiable and accurately learn the pivotal regions distributed randomly in the input images, we represent the anchor tokens with neurons and utilize the neural layer to fit the distribution.
- Inspired by the Markov process, the global similarities can be obtained from the distribution of anchors. Meanwhile, by rearranging the multiplication orders, it obtain the linear complexity such as $\mathcal{O}(mn)$. Extensive experiments show the effectiveness of the proposed model, i.e., 9.0% higher accuracy or 46.7% FLOPs reduction on classification.

2. Related Work

2.1. Vision Transformers

Recently, by introducing the multi-head self-attention mechanism to extract the intrinsic features, transformers have shown excellent performance on sequential tasks such as natural language processing [9, 18, 49]. Inspired by its

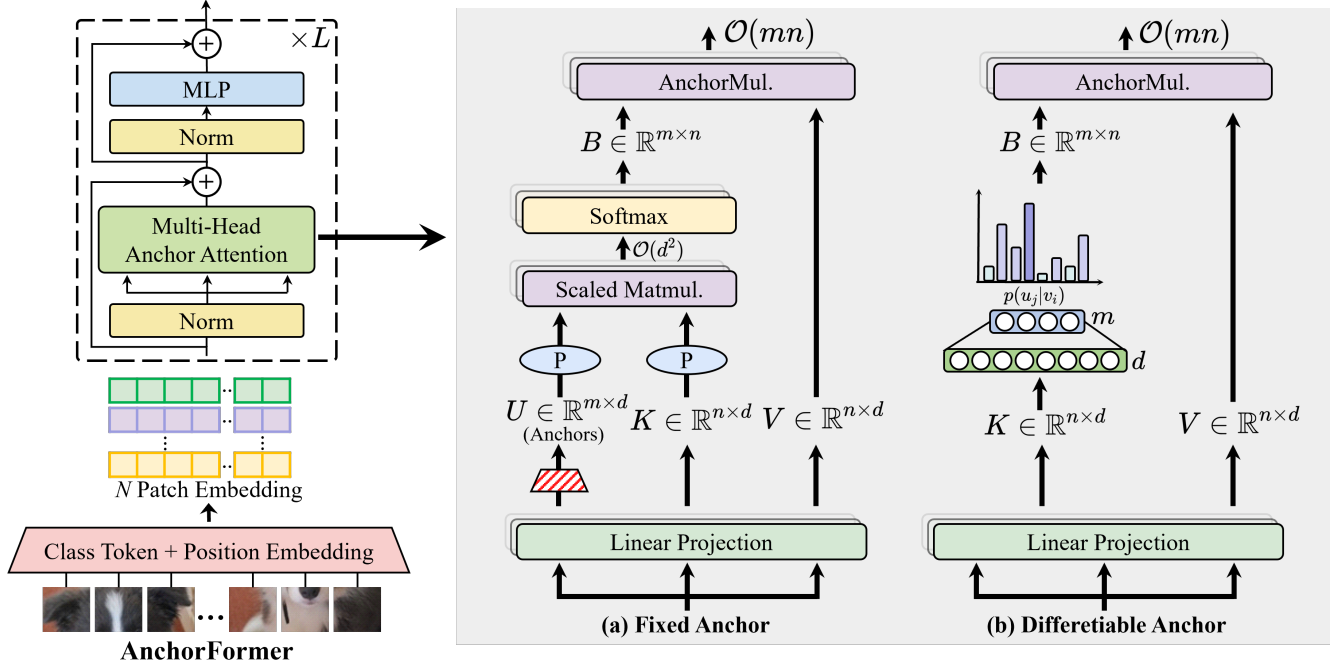


Figure 3. The architecture of the proposed AnchorFormer. AnchorFormer has L multi-head anchor attention layers. It splits the input image into n patches. Fig. (a) is the proposed basic anchor-based attention layer. It selects m anchors among the queries Q and calculates the pivotal similarities. Fig. (b) utilizes a deep neural layer to represent m anchors and differentiable learn the pivotal similarities. The block is named **AnchorMul**, can learn the global attention based on the Markov process.

success, some researchers attempt to study similar models on image processing and vision tasks. As a mainstream model, a vision transformer (ViT) introduces a small granularity to group the pixels into a series of patches and directly extend the transformer on these patches for image classification [11]. It obtains a modest accuracy on ImageNet than the ResNets with comparable size. Having pretrained on more large datasets (>14 million), ViT can achieve excellent performance and even exceed some state-of-the-art baselines. [48] designs a convolution free transformer (DeiT) only trained on ImageNet. DeiT-B has the same parameters as ViT-B and achieves 83.1% top-1 accuracy. Following the structure of ViTs, a series of ViTs variants have been designed for vision tasks. Among them, some researchers attempt to study the improvement of ViTs in extracting local information [6, 17, 29]. TNT further divides the patches into some sub-patches and designs the inner transformer blocks to model the relationship between them [17]. Swin transformer introduces the shift windows to explore the connection between the local features [29]. Besides, modifying the interaction among each attention head also attracts many researchers. DeepViT introduces a cross-head communication mechanism to relearn the feature map and increase the performance [69]. XCiT calculates the attention map across the different feature channels

instead of tokens, which can extend the ViTs on more high-resolution inputs [1].

Although ViTs and their variants have achieved excellent performance on many vision tasks, their complexity grows quadratically with the number of input tokens such as $\mathcal{O}(n^2)$. It will take excessive computation costs and be impractical to extend on the device with limited memory consumption.

2.2. Efficient Vision Transformers

In this section, we review some works carried out to improve the efficiency and accelerating the transformers. Firstly, some researchers introduce the pruning and decomposition strategies. [31] proves that all attention heads are not required for specific downstream tasks. It removes some heads and reduces the model parameters by estimating the influence of each head on the final output. Meanwhile, some works attempt to reduce the depths instead of the width of transformers [12, 20]. Apart from the pruning, matrix decomposition is also employed to improve the efficiency [53]. Secondly, knowledge distillation also is utilized to improve efficiency. [32] utilizes a pre-trained BERT model as the teacher to guide the student transformer training. For vision transformers, [22] introduces the manifold learning into the distillation to explore the relation-

ship among the patches and improve performance. Thirdly, there is a lot of work on how to introduce quantization in transformers [3, 30]. [42] represents the input with binary high-dimensional vectors and reduces the complexity. [36] proposes a fully quantized transformer to handle the machine translation tasks. Lastly, more researchers pay attention to designing compact transformer architecture. Our model also belongs to this category. The neural architecture search (NAS) is introduced to automatically search for the best compact architecture [16, 43]. Inspired by the graph theory, some models introduce sparsity in estimating the similarity among the tokens [44, 52, 63]. However, these methods may discard some informative features due to constructing the sparse attention. Although the slide windows based strategy can solve this problem and reduce the complexity simultaneously [10, 29], the window attention introduces an extra obstacle to cross-window communication. In this paper, we propose a new insight to accelerate the ViTs with anchor tokens, which can not only significantly reduce the parameters and computation complexity but also enhance the learning for pivotal information.

3. Method

To learn the pivotal information and improve the efficiency, we introduce an anchor-based vision transformer (**AnchorFormer**) framework in this section. It can reduce the complexity from $\mathcal{O}(n^2)$ to $\mathcal{O}(mn)$ by estimating the bipartite attention between anchors and other tokens, where m is the number of tokens. Furthermore, we design a neural layer to represent the anchors and differentiable learn the pivotal information for inference. The framework is illustrated in Fig. 3.

3.1. Motivation

Recently, vision transformers (ViTs) have shown impressive performance on vision tasks. As a core component of ViTs, the self-attention module generally consists of multiple heads [61]. Given n tokens, each head can capture the global information by measuring the similarities among all tokens as

$$h_t^m = \sum_{i=1}^n \frac{\exp(q_t k_i^T / \sqrt{d})}{\sum_{j=1}^n \exp(q_t k_j^T / \sqrt{d})} v_i, \quad (1)$$

where $q_t \in Q$, $k_i \in K$, $v_i \in V$, $h_t \in H$ are the row vectors, $\exp(\cdot)$ is an exponential function, and m is the m -th head. $H \in \mathbb{R}^{n \times d}$ is an attention matrix. $Q, K, V \in \mathbb{R}^{n \times d}$ are the query, key, and value. They are both obtained by projecting the tokens $X \in \mathbb{R}^{n \times D}$ with three learnable weights $W^Q, W^K, W^V \in \mathbb{R}^{D \times d}$. Eq. (1) estimates the similarities between each pair of tokens by calculating the inner product between the query-key pairs, which has $\mathcal{O}(n^2)$ complexity and takes the vast costs. Besides, enlightened

that the pivotal information of the input image often randomly gathers in a few regions, the model could pay more attention to the similarities among these regions. To sum up, there is a natural question, *how to efficiently accelerate the ViTs for learning the pivotal similarities?*

3.2. Accelerate ViTs with Anchor Tokens

In this work, the distributions among the tokens are denoted by the conditional probability such as $p(v_j|v_i)$. Correspondingly, the similarities between them can be viewed as the sampling results from $p(v_j|v_i)$. Thus, the global similarities learned by vanilla ViTs is reformulated as

$$p(v_j|v_i) = \frac{\exp(q_j k_i^T / \sqrt{d})}{\sum_{j=1}^n \exp(q_j k_i^T / \sqrt{d})}, \quad (2)$$

where $\sum_{j=1}^n p(v_j|v_i) = 1$ and $p(v_j|v_i) = p(v_i|v_j)$. As shown in Eq. (2), vanilla ViTs mainly compute the inner products between the query Q and the key K to measure the global self-attention. Thus, to accelerate the ViTs, a direct insight is selecting some representative tokens named **anchors** $U \in \mathbb{R}^{m \times d}$, where m is the number of anchors [64]. Then, to obtain the global self-attention H and accelerate the ViTs, we not only need to obtain the pivotal distributions as $p(v_j|u_i)$ but also attempt to estimate the global distributions $p(v_j|v_i)$ from them.

Specifically, the pivotal similarities between anchors and tokens can be viewed as sampling results from $p(u_j|v_i)$. Meanwhile, since the anchors indicate the more representative tokens, the ideal anchors should satisfy the following problem as

$$\min_{u, p(\cdot|v_i)} \sum_{i=1}^n \mathbb{E}_{u \sim p(\cdot|v_i)} \text{dist}(u, v_i), \quad (3)$$

where $\text{dist}(u, v_i)$ mainly measures the distance between the anchors and other tokens. Notably, we take the same inner product and normalized strategy as vanilla ViTs to obtain $p(u_j|v_i)$,

$$p(u_j|v_i) = \frac{\exp(u_j k_i^T / \sqrt{d})}{\sum_{j=1}^m \exp(u_j k_i^T / \sqrt{d})}, \quad (4)$$

where $p(u_j|v_i) = p(v_i|u_j)$. Meanwhile, following vanilla ViTs, we also introduce k_i to measure the relationship between the tokens. Correspondingly, Eq. (3) is reformulated as

$$\min_{u, p(\cdot|v_i)} \sum_{i=1}^n \mathbb{E}_{u \sim p(\cdot|v_i)} \|u - k_i\|_2^2. \quad (5)$$

Then, the anchors can be solved by taking the derivative of Eq. (5) regarding u and setting it to 0,

$$u = \frac{\sum_{i=1}^n p(u|v_i) k_i}{\sum_{i=1}^n p(u|v_i)}. \quad (6)$$

To estimate the bipartite attention between anchors and all tokens, we further reformulate $p(\mathbf{u}_j|\mathbf{v}_i)$ and $p(\mathbf{v}_i|\mathbf{u}_j)$ by matrix form. Let $\mathbf{A} \in \mathbb{R}^{n \times m}$ be a matrix where $a_{ij} = p(\mathbf{u}_j|\mathbf{v}_i)$ as Eq. (4),

$$\mathbf{G} = \begin{bmatrix} \mathbf{0} & \mathbf{A} \\ \mathbf{A}^T & \mathbf{0} \end{bmatrix}, \mathbf{D} = \begin{bmatrix} \mathbf{I} & \mathbf{0} \\ \mathbf{0} & \mathbf{\Delta} \end{bmatrix}, \quad (7)$$

where \mathbf{D} is a diagonal matrix and $d_{ii} = \sum_{j=1}^{n+m} t_{ij}$. To bridge the anchors and all tokens, we introduce a probability transferring matrix as

$$\mathbf{F} = \mathbf{D}^{-1} \mathbf{G} = \begin{bmatrix} \mathbf{0} & \mathbf{A} \\ \mathbf{\Delta}^{-1} \mathbf{A}^T & \mathbf{0} \end{bmatrix} \in \mathbb{R}^{(n+m) \times (n+m)}. \quad (8)$$

Then, according to the Markov process [2], $p(\mathbf{v}_j|\mathbf{v}_i)$ can be estimated by the one-step transition probability as

$$p(\mathbf{v}_j|\mathbf{v}_i) = \sum_{l=1}^m p(\mathbf{v}_j|\mathbf{u}_l) p(\mathbf{u}_l|\mathbf{v}_i). \quad (9)$$

Similarly, $p(\mathbf{u}_j|\mathbf{u}_i) = \sum_{l=1}^n p(\mathbf{u}_j|\mathbf{v}_l) p(\mathbf{v}_l|\mathbf{u}_i)$. Thus, the one-step transition probability is formulated as

$$\mathbf{F}^2 = \begin{bmatrix} \mathbf{A} \mathbf{\Delta}^{-1} \mathbf{A}^T & \mathbf{0} \\ \mathbf{0} & \mathbf{\Delta}^{-1} \mathbf{A}^T \mathbf{A} \end{bmatrix} = \begin{bmatrix} \mathbf{S}_t & \mathbf{0} \\ \mathbf{0} & \mathbf{S}_u \end{bmatrix}, \quad (10)$$

where \mathbf{S}_t indicates the self-attention among n tokens, constructed by m anchors, and \mathbf{S}_u shows the similarities between the anchors. Besides, \mathbf{S}_t has been normalized because of

$$\mathbf{S}_t \mathbf{1}_n = \mathbf{A} \mathbf{\Delta}^{-1} \mathbf{A}^T \mathbf{1}_n = \mathbf{1}_n, \quad (11)$$

where $\mathbf{1}_n \in \mathbb{R}^{n \times 1}$. Thus, the global similarities among the tokens are the sampling results of \mathbf{S}_t and the global self-attention \mathbf{H} is calculated by

$$\mathbf{H} = \mathbf{A} \mathbf{\Delta}^{-1} \mathbf{A}^T \mathbf{V}. \quad (12)$$

Then, we explain how Eq. (12) accelerates the ViTs. It should be emphasized that \mathbf{S}_t cannot be calculated explicitly. The core idea is to **rearrange the multiplication order**,

$$\mathbf{M}_1 = \mathbf{B}^T \mathbf{V} \Rightarrow \mathbf{M}_2 = \mathbf{\Delta}^{-1} \mathbf{M}_1 \Rightarrow \mathbf{M}_3 = \mathbf{B} \mathbf{M}_2, \quad (13)$$

where the complexity of \mathbf{M}_1 , \mathbf{M}_2 and \mathbf{M}_3 are $\mathcal{O}(mnd)$, $\mathcal{O}(m^2d)$, and $\mathcal{O}(nmd)$, respectively. Thus, the computational complexity of Eq. (13) is $\mathcal{O}(nmd + m^2d)$. Because m and d generally are smaller than n , the complexity is reduced to $\mathcal{O}(nm)$. More importantly, if the number of anchors is small enough, we just take $\mathcal{O}(n)$ to obtain global self-attention.

3.3. AnchorFormer: Differentiable Anchor ViTs

Since the pivotal information is often randomly gathered in the input images, an ideal strategy is utilizing the neural layer to fit their distributions and differentiable learn the pivotal similarities \mathbf{B} . Meanwhile, indicated by Eq. (13), the global self-attention \mathbf{H} is directly dependent on the pivotal similarities. Thus, we design an anchor transformer (AnchorFormer) that focuses on differentiable learning the pivotal similarities in attention heads.

Specifically, we generate the keys \mathbf{K} and the values \mathbf{V} by two learnable parameters \mathbf{W}^K and \mathbf{W}^V , respectively. Notably, to extract the deep information, a neural layer generally in a deep neural network (DNN) introduces a learnable projection matrix and calculates the inner product between it and the input data. Inspired by it, Eq. (4) can be fitted with a neural layer as

$$p(\mathbf{u}_j|\mathbf{v}_i) = \frac{\exp(\mathbf{w}_j^S \mathbf{k}_i^T / \sqrt{d})}{\sum_{j=1}^n \exp(\mathbf{w}_j^S \mathbf{k}_i^T / \sqrt{d})}, \quad (14)$$

where $\mathbf{w}_j^S \in \mathbb{R}^{m \times d}$ is an anchor and can be implemented by learnable parameters. Thus, the pivotal similarities $p(\mathbf{u}_j|\mathbf{v}_i)$ can be learned differentiable and the learnable anchors can accurately mine the latent distribution of the pivotal region for whole input images by gradient descent. Since the proposed anchor-based attention can be calculated independently, it can naturally be extended to multi-head self-attention learning. Among them, each head can capture the global self-attention by Eq. (14) and Eq. (13). Then, for l heads, the global multi-head self-attention is calculated by

$$\mathbf{H}^M = (\mathbf{H}^1 \oplus \mathbf{H}^2 \oplus \dots \oplus \mathbf{H}^l) \mathbf{W}, \quad (15)$$

where $\mathbf{W} \in \mathbb{R}^{ld \times d}$ is a projection matrix and \oplus is the matrix concatenation operation.

Furthermore, compared to vanilla ViTs, the proposed AnchorFormer not only can accelerate the ViTs by introducing the anchor tokens but also effectively reduce the space complexity thanks to differentiable estimate the pivotal similarities. Meanwhile, as shown in the experiment section, the proposed model can achieve up to **46.7%** FLOPs reduction on ImageNet classification. Especially, since exploring the pivotal information distribution among the whole datasets, the classification accuracy also be improved.

4. Experiments

In this paper, we design an anchor-based efficient vision transformer (**AnchorFormer**) to reduce the computational complexity of ViT and focus on learning the pivotal information. Thus, the experiments mainly verify the efficiency and performance of AnchorFormer on three downstream tasks including classification, detection, and segmentation.

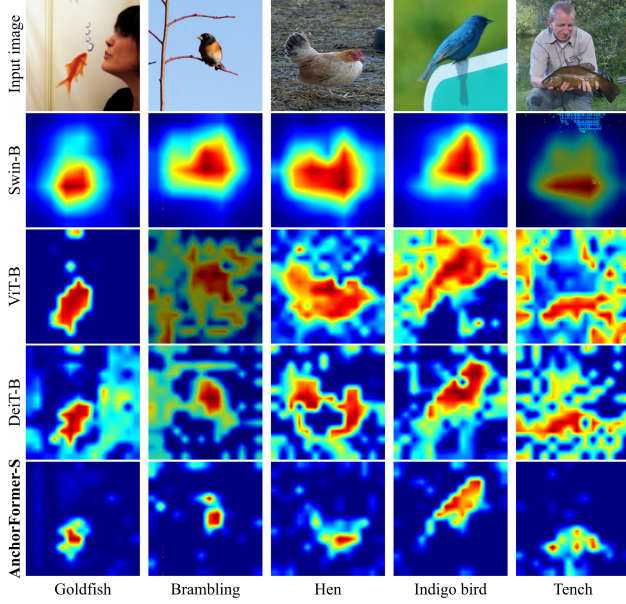


Figure 4. Visual explanations generated by different models on the ImageNet validation dataset [8]. From top to down: input image, visual explanation maps of the Swin-B [29], ViT-B, DeiT-B [48] and our AnchorFormer-S, respectively.

4.1. Experimental Settings

4.1.1. Datasets and Tasks

To verify the performance and efficiency of the proposed model, we introduce three representative datasets and three mainstream computer vision tasks, i.e., image classification on the ImageNet dataset [8], object detection on the COCO dataset [28], and semantic segmentation on ADE210K [68]. Among them, the ImageNet dataset contains 1.41M real images with 1K categories. The training set, validation set and test set have 1.28M, 50K and 100K images, respectively. The COCO dataset has 118K training images and 5K testing images with 80 object classes. ADE210K dataset has 20K training images, 2K validation images, and 3K testing images. Meanwhile, we will extend the proposed AncorFormer to the representative models. It is extended on the DeiT [48] for the classification. We introduce the PicoDet [62] as the backbones and equip the LCNet [7] with the proposed model for detection. For segmentation, we introduce the Semantic-FPN [24] and UperNet [57] as the backbone.

4.1.2. Comparative Methods

For the classification, we introduce several current efficient deep models as the baseline. It includes EfficientNet [46], LeViT [15], DeiT [48], AutoFormer [5], Swin [29], CSWin [10], MViTv2 [27], PVT [52], CastlingViT [61], BiFormer [70] and SlideFormer [34]. Besides, three sparse attention based ViT, Sparsifiner [54], Combiner [40] and ClusterFormer [51], are also employed as baselines. For object detection, five famous detection models are employed as the

FLOPs Ranges	Models	Params (M)	FLOPs (G)	Top-1 Acc.(%)	Top-5 Acc.(%)
<1G	EfficientNet-B0	5.3	0.4	77.05	<u>91.27</u>
	EfficientNet-B1	7.8	0.7	78.32	90.72
	LeViT-128	9.2	0.4	78.33	89.18
	LeViT-192	10.9	0.7	<u>80.13</u>	90.53
	CastlingViT-192	12.7	0.8	79.73	<u>91.27</u>
	AnchorFormer-T	4.2	0.7	81.12	93.86
1~5G	Sparsifiner	4.2	1.3	74.38	91.97
	Combiner	6.4	1.5	68.37	76.81
	Sparsifiner	5.3	1.8	64.72	73.74
	EfficientNet-B3	12.3	1.8	81.54	94.85
	EfficientNet-B4	19.1	4.2	82.83	96.43
	DeiT-T	5.6	1.3	74.38	91.97
	DeiT-S	21.9	4.6	81.58	95.06
	LeViT-256	18.9	1.1	81.53	94.17
	LeViT-384	39.1	2.4	82.17	95.36
	Swin-T	29.6	4.5	80.94	94.33
	CSWin-T	23.4	4.3	82.22	93.46
	PVTv2-V2	25.5	4.2	81.86	93.65
	MViTv2-T	24.1	4.7	82.21	94.16
	CastlingViT-384	45.8	2.9	83.26	<u>96.69</u>
	SlideFormer-T	12.2	2.6	77.51	91.67
	SlideFormer-S	22.7	4.5	81.75	92.48
	BiFormer-T	13.1	2.2	81.32	93.31
	BiFormer-S	26.4	4.5	<u>83.89</u>	93.86
	AnchorFormer-S	18.6	2.7	84.69	96.82
>5G	EfficientNet-B5	30.7	9.9	83.64	96.13
	DeiT-B	86.3	17.5	83.21	96.13
	Swin-S	50.3	8.7	83.16	<u>96.17</u>
	Swin-B	88.1	15.4	83.51	96.14
	CSWin-S	35.6	6.9	83.57	95.75
	CSWin-B	78.3	15.2	84.22	96.14
	AutoFormer-S	22.9	5.1	81.72	95.73
	AutoFormer-B	54.8	11.7	82.47	95.64
	MViTv2-S	34.7	6.9	83.56	94.71
	MViTv2-B	51.2	10.1	84.37	95.06
	CastlingViT-S	34.7	7.3	84.63	95.36
	CastlingViT-B	87.2	17.3	<u>84.82</u>	95.87
	SlideFormer-B	89.7	15.5	84.42	96.07
	BiFormer-B	58.3	9.8	84.13	95.88
	AnchorFormer-B	63.5	9.2	86.62	97.84

Table 1. Classification on ImageNet Dataset. The baselines are divided into three categories according to the FLOPs. The last column represents the Top-1 improvements of each model than three baselines including LeViT-192, DeiT-S and DeiT-B.

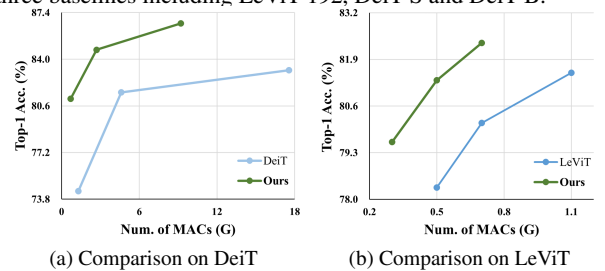


Figure 5. AnchorFormer vs. baseline on ImageNet. Fig. 5a shows the achievement than DeiT and Fig. 5b shows the improvements than LeViT.

baselines, i.e., YOLOv5, YOLOX [14], EfficientDet [47], MobileDet [58], FBNetV5 [55] and the current CastlingViT.

Models	Params (M)	FLOPs (G)	mAP	AP50	AP75
YOLOv5-N	1.9	4.5	28.38	45.21	-
YOLOv5-S	7.2	16.5	35.18	52.55	-
YOLOX-Nano	0.91	0.54	25.23	-	-
YOLOX-Tiny	5.06	3.23	32.37	-	-
EfficientDet-512	3.9	2.5	33.81	52.24	35.82
EfficientDet-640	6.6	6.1	39.58	58.59	42.28
EfficientDet-768	8.1	10.8	<u>43.25</u>	<u>62.31</u>	<u>46.18</u>
MobileNetV2	4.3	1.2	22.13	-	-
MobileNetV3	3.3	1.5	23.48	-	-
FBNetV5-A	-	1.4	27.35	-	-
FBNetV5- A_C	-	1.4	28.98	-	-
FBNetV5- A_R	-	1.8	30.52	-	-
CastlingViT-S	3.3	1.1	31.34	46.69	32.52
CastlingViT-M	6.0	2.0	34.07	49.63	35.83
CastlingViT-L	13.1	5.3	34.42	53.59	39.58
AnchorFormer-T	2.9	1.1	41.23	60.57	45.46
AnchorFormer-S	5.5	1.7	43.61	62.83	48.29
AnchorFormer-B	8.6	2.8	45.75	65.35	51.81

Table 2. AnchorFormer over SOTA detection baselines on the COCO dataset, where the proposed model replaces the last stage of ESNet. “-T/S/B” and “-512/640/768” mean tiny/small/base and different input resolution, respectively.

For the semantic segmentation, we introduce ResNet [19], PVT [52], Swin [29], DAT [56], Focal [60], RMT [13] and GraftViT [35] as baselines.

4.1.3. Settings and Metrics

To be fair, the proposed model and the comparative methods are trained with the same settings. For the classification task, we employ a SGD optimizer to train each model for 300 epochs using 8 Nvidia RTX 4090Ti GPUs and the batch size is 256. The learning rate is $5e^{-4}$, the momentum is 0.9 and the weight decay is 0.05. The distillation-based models employ RegNetY [38] as the teacher network. For the detection task, we utilize the SGD to train the model on the COCO dataset with 300 epochs. The learning rate is 0.01. The other setting is the same as PicoDet [62]. For the segmentation task, the training setting is the same as Maskformer. For our model, the number of anchors is 30. Besides, we evaluate the model on these tasks from the accuracy and efficiency. Among them, the efficiency metrics contain the number of parameters (**Params**) and the inference FLOPs (**FLOPs**). The accuracy metrics contain **Top-1/5** for classification, **AP**, **AP⁵⁰**, **AP⁷⁵** for detection, and **mIoU**, **mAcc** for segmentation.

4.2. Visualization and analysis

To make the proposed more explanation, we utilize the Grad-CAM [41] to visualize and show the deep feature maps of the proposed method and some representative baselines including Swin [29], vanilla ViT, and DeiT. Fig. 4 suggests the visual comparison based on randomly chosen im-

ages from the ImageNet validation. As can be shown from the figures, these models can make the higher attention on the target area corresponding the category. Compared with the Swin, the ViT-based models can notice the outline or shape of the target category. More importantly, thanks to differentiable learning of the pivotal information with the anchor tokens, the proposed AnchorFormer can distinguish and pay more attention to the target area from the global receptive field, which significantly improves performance. Notably, according to Table 1, the parameters and FLOPs of our AnchorFormer-S are much lower than the comparative baselines including Swin-B, ViT-B and DeiT-B. It proves that the anchor mechanism can alleviate some redundant parameters to improve the performance and reduce the model size, simultaneously.

4.3. Image Classification

To evaluate the performance on the classification task, we extend our AnchorFormer on the representative vision transformer architecture as DeiT [48] with different sizes and compare their performance over some current baselines on the ImageNet dataset. The results are listed in Table 1. For clarity, all methods are divided into three categories according to the FLOPs range: $< 1G$, $1 \sim 5G$, and $> 5G$. Across the different FLOPs ranges, AnchorFormer consistently achieves the best performance than the others in terms of accuracy and efficiency. For instance, AnchorFormer-B obtains 86.62% top-1 accuracy with 9.2G FLOPs while the current BiFormer-B takes 15.5G FLOPs to achieve 84.42% accuracy, i.e., $\downarrow 40.6\%$ FLOPs and $\uparrow 2.6\%$ accuracy. Besides, under comparable FLOPs, AnchorFormer-S obtains 84.69% top-1 accuracy with 2.7G FLOPs and BiFormer-S has 83.89% accuracy with 4.5G FLOPs, i.e., $\downarrow 40.0\%$ FLOPs and $\uparrow 1.0\%$ performance. In a word, the proposed model has improved the top-1 accuracy of $\uparrow 1.2\% \sim \uparrow 5.3\%$, $\uparrow 1.0\% \sim \uparrow 13.9\%$, and $\uparrow 2.1\% \sim \uparrow 6.0\%$ than the other baselines under $< 1G$ FLOPs, $1 \sim 5G$ FLOPs, and $> 5G$ FLOPs, respectively. Furthermore, we also introduce the comparative experiments on the apple-to-apple benchmark including, DeiT vs. AnchorDeiT, and LeViT vs. AnchorLeViT. In Fig. 5, compared with DeiT, ours achieves $\downarrow 41.3\% \sim \downarrow 46.7\%$ FLOPs reductions and $\uparrow 3.8\% \sim \uparrow 9.0\%$ better accuracy. Compared with LeViT, AnchorFormer obtains $\downarrow 28.5\% \sim \downarrow 40.0\%$ FLOPs reductions and $\uparrow 1.0\% \sim \uparrow 1.6\%$ better accuracy.

4.4. Object Detection

Meanwhile, to verify the efficiency of the downstream object task, we extend AnchorFormer on the COCO dataset and introduce some efficient detection models as the baselines. Specifically, we employ ESNet [62] as the backbone and replace the last stage with the proposed AnchorFormer. Meanwhile, the detector head and the training

Backbone	Method	Params (M)	FLOPs (G)	mIoU (%)	mACC (%)
ResNet50	Semantic-FPN	28.5	183.2	36.75	43.88
PVT	Semantic-FPN	29.5	221.6	42.83	52.15
Swin	Semantic-FPN	31.9	182.3	41.56	51.42
DAT	Semantic-FPN	32.3	198.8	42.63	54.72
AnchorFormer	Semantic-FPN	21.6	193.7	43.81	56.57
Swin	UperNet	57.3	945.8	45.28	54.32
Focal	UperNet	62.3	998.1	45.8	52.62
RMT	UperNet	56.4	937.4	49.8	-
GraftViT	UperNet	66.4	954.6	45.5	53.2
AnchorFormer	UperNet	49.6	928.1	46.28	56.33

Table 3. AnchorFormer over segmentation baselines on the ADE210K dataset, where we extend the proposed AnchorFormer on two segmentation methods, Semantic-FPN and UperNet. The resolution of the input image is 512×2048 .

ViT	Anchor	Diff.	Params (M)	FLOPs (G)	Top-1 (%)	Improv. (%)
✓			6.3	1.5	72.51	2.58 (↓)
✓	✓		4.7	0.9	77.48	4.00 (↑)
✓	✓	✓	4.2	0.7	81.12	8.31 (↑)
DeiT-T			5.6	1.3	74.38	0.00 (↑)

Table 4. Ablation study of the proposed AnchorFormer with different designed parts. The ViT means the vanilla ViT baseline. They are conducted on the ImageNet dataset for classification. The last column represents the Top-1 improvements of each model than DeiT-T baseline.

settings are followed by PicoDet. The comparative results are listed in Table 2. We can find that ours consistently obtains the best trade-off between accuracy and efficiency, i.e., $\uparrow 30.0\% \sim \uparrow 81.3\%$, $\uparrow 6.4\% \sim \uparrow 35.3\%$, and $\uparrow 49.9\% \sim \uparrow 67.3\%$ mAP improvements compared to YOLO, EfficientDet and FBNetV5, respectively, under comparable FLOPs. Our mAP is far higher than the detection based on MobileNet under comparable parameters. Especially for the baselines of YOLO and MobileNet, the proposed AnchorFormer-T can achieve the highest mAP with the smallest FLOPs. It is mainly because that the proposed model can differentiable learn the pivotal information distributed randomly among the image dataset. Thus, we can achieve the best trade-off performance and efficiency on the downstream object detection task.

4.5. Semantic Segmentation

Furthermore, we extend the proposed AnchorFormer on the semantic segmentation task and verify the performance and efficiency. We employ the Semantic-FPN [24] and UperNet [57] as the backbones of the ADE210K dataset. As shown in Table 3, the proposed model achieves better performance than the baselines in terms of accuracy and efficiency. Among them, our AnchorFormer obtains $\downarrow 14.4\%$ FLOPs reduction and $\uparrow 2.3\%$ mIoU improvement than

Anchor Num.				Params (M)	FLOPs (G)	Top-1 (%)	Improv. (%)
10	30	50	100				
✓				3.9	0.6	77.25	3.72 (↑)
	✓			4.2	0.7	81.12	8.31 (↑)
		✓		4.3	0.8	79.62	6.58 (↑)
			✓	4.7	1.0	75.83	1.91 (↑)
DeiT-T				5.6	1.3	74.38	0.00 (↑)
✓				15.3	2.4	81.73	0.18 (↑)
	✓			18.6	2.7	84.69	3.67 (↑)
		✓		19.1	2.9	82.16	0.71 (↑)
			✓	19.4	3.2	80.69	1.10 (↓)
DeiT-S				21.9	4.6	81.58	0.00 (↑)

Table 5. Ablation study of the proposed AnchorFormer with the different number of anchors. The experiments are conducted on DeiT-S and DeiT-B for ImageNet classification. The last column represents the Top-1 improvements of each model than DeiT-T and DeiT-S baselines, respectively.

PVT. The proposed model obtains $\downarrow 1.88\%$ FLOPs reduction and $\uparrow 2.2\%$ mIoU improvement than Swin. This experiments proves that our AnchorFormer can be generalized to various vision tasks and achieve excellent performance.

4.6. Ablation Study

To validate the effectiveness of the designs including anchor vision transformer (**Anchor**) and differentiable anchor vision transformer (**Diff.**), we conduct several ablation studies on image classification tasks. Specifically, we conduct them on the ImageNet dataset and employ the vanilla ViT and DeiT as the baselines. As shown in Table 4, the differentiable anchor vision transformer achieves better performance than the others in terms of accuracy and efficiency. Compared with the basic anchor vision transformer, the differentiable model obtains $\downarrow 22.2\%$ FLOPs reduction and $\uparrow 4.5\%$ top-1 accuracy improvement. It suggests that the proposed model can accurately and differentiable learn the pivotal information among the input image dataset.

Besides, we also conduct ablation experiments to study the sensitivity of the different numbers of anchors. The two architectures, DeiT-T and DeiT-S, are employed. The number of anchors is selected from [10, 30, 50, 100]. As shown in Table 5, more and less number of anchors may not achieve the highest performance on ImageNet classification. Specifically, under comparable FLOPs, AnchorFormer with 30 anchors obtains $\uparrow 4.8\%$ and $\uparrow 3.5\%$ than AnchorFormer with 10 on DeiT-T and DeiT-S, respectively. It means that too less anchors may discard some features and drop the performance. AnchorFormer with 30 anchors achieves FLOPs reduction and top-1 accuracy improvement simultaneously than AnchorFormer with 100 anchors. It means that too many anchors also introduce redundant information to limit the performance. Therefore, we can simply set the anchor number as a median like 30.

5. Conclusion

In this paper, we propose an anchor-based efficient vision transformer to learn the pivotal information with the anchor tokens and accelerate the inference of ViTs. It mainly estimates the bipartite attention between the anchors and the tokens to reduce the complexity. Notably, these anchors can be represented as neurons in a neural layer. Thus, we can differentiable learn global self-attention through the Markov process and the complexity will be reduced to $\mathcal{O}(mn)$, where m is an anchor number and $m < n$. Moreover, extensive experiments can verify the performance and efficiency of our model. Especially, it achieves up to a **9.0%** higher accuracy or **46.7%** FLOPs reduction than other current baselines on the ImageNet classification. Meanwhile, we believe that the proposed anchor-based strategy opens up a new perspective on efficiency improvement. In the future, it is also promising to further improve the proposed method by using positive-incentive noise theory [25] since the anchor attention can be regarded as a noisy approximation of the vanilla attention. The positive-incentive noise [25] is the first mathematical framework to quantify the noise impact. The novel concept shows us how to systematically study the noise and the following series of works [21, 59, 65, 66] shows us how to effectively apply the elegant framework to the popular deep learning models.

References

- [1] Alaaeldin Ali, Hugo Touvron, Mathilde Caron, Piotr Bojanowski, Matthijs Douze, Armand Joulin, Ivan Laptev, Natalia Neverova, Gabriel Synnaeve, Jakob Verbeek, et al. Xcit: Cross-covariance image transformers. *Advances in neural information processing systems*, 34:20014–20027, 2021. 3
- [2] Charles Ames. The markov process as a compositional model: A survey and tutorial. *Leonardo*, 22(2):175–187, 1989. 5
- [3] Aishwarya Bhandare, Vamsi Sripathi, Deepthi Karkada, Vivek Menon, Sun Choi, Kushal Datta, and Vikram Sale-tore. Efficient 8-bit quantization of transformer neural machine language translation model. *arXiv preprint arXiv:1906.00532*, 2019. 4
- [4] Nicolas Carion, Francisco Massa, Gabriel Synnaeve, Nicolas Usunier, Alexander Kirillov, and Sergey Zagoruyko. End-to-end object detection with transformers. In *European conference on computer vision*, pages 213–229. Springer, 2020. 1
- [5] Minghao Chen, Houwen Peng, Jianlong Fu, and Haibin Ling. Autoformer: Searching transformers for visual recognition. In *Proceedings of the IEEE/CVF international conference on computer vision*, pages 12270–12280, 2021. 2, 6
- [6] Richard Chen, Rameswar Panda, and Quanfu Fan. Regional-to-local attention for vision transformers, 2024. US Patent 11,915,474. 3
- [7] Cheng Cui, Tingquan Gao, Shengyu Wei, Yuning Du, Ruoyu Guo, Shuilong Dong, Bin Lu, Ying Zhou, Xueying Lv, Qiwen Liu, et al. Pp-lcnet: A lightweight cpu convolutional neural network. *arXiv preprint arXiv:2109.15099*, 2021. 6
- [8] Jia Deng, Wei Dong, Richard Socher, Li-Jia Li, Kai Li, and Li Fei-Fei. Imagenet: A large-scale hierarchical image database. In *2009 IEEE conference on computer vision and pattern recognition*, pages 248–255. Ieee, 2009. 6
- [9] Jacob Devlin. Bert: Pre-training of deep bidirectional transformers for language understanding. *arXiv preprint arXiv:1810.04805*, 2018. 2
- [10] Xiaoyi Dong, Jianmin Bao, Dongdong Chen, Weiming Zhang, Nenghai Yu, Lu Yuan, Dong Chen, and Baining Guo. Cswin transformer: A general vision transformer backbone with cross-shaped windows. In *Proceedings of the IEEE/CVF conference on computer vision and pattern recognition*, pages 12124–12134, 2022. 2, 4, 6
- [11] Alexey Dosovitskiy, Lucas Beyer, Alexander Kolesnikov, Dirk Weissenborn, Xiaohua Zhai, Thomas Unterthiner, Mostafa Dehghani, Matthias Minderer, Georg Heigold, Sylvain Gelly, et al. An image is worth 16x16 words: Transformers for image recognition at scale. *arXiv preprint arXiv:2010.11929*, 2020. 1, 3
- [12] Angela Fan, Edouard Grave, and Armand Joulin. Reducing transformer depth on demand with structured dropout. *arXiv preprint arXiv:1909.11556*, 2019. 3
- [13] Qihang Fan, Huaibo Huang, Mingrui Chen, Hongmin Liu, and Ran He. Rmt: Retentive networks meet vision transformers. In *Proceedings of the IEEE/CVF Conference on Computer Vision and Pattern Recognition*, pages 5641–5651, 2024. 7
- [14] Zheng Ge, Songtao Liu, Feng Wang, Zeming Li, and Jian Sun. YoloX: Exceeding yolo series in 2021. *arXiv preprint arXiv:2107.08430*, 2021. 6
- [15] Benjamin Graham, Alaaeldin El-Nouby, Hugo Touvron, Pierre Stock, Armand Joulin, Hervé Jégou, and Matthijs Douze. Levit: a vision transformer in convnet’s clothing for faster inference. In *Proceedings of the IEEE/CVF international conference on computer vision*, pages 12259–12269, 2021. 2, 6
- [16] Yong Guo, Yin Zheng, Minghui Tan, Qi Chen, Jian Chen, Peilin Zhao, and Junzhou Huang. Nat: Neural architecture transformer for accurate and compact architectures. *Advances in Neural Information Processing Systems*, 32, 2019. 4
- [17] Kai Han, An Xiao, Enhua Wu, Jianyuan Guo, Chunjing Xu, and Yunhe Wang. Transformer in transformer. *Advances in neural information processing systems*, 34:15908–15919, 2021. 3
- [18] Kai Han, Yunhe Wang, Hanting Chen, Xinghao Chen, Jianyuan Guo, Zhenhua Liu, Yehui Tang, An Xiao, Chunjing Xu, Yixing Xu, et al. A survey on vision transformer. *IEEE transactions on pattern analysis and machine intelligence*, 45(1):87–110, 2022. 2
- [19] Kaiming He, Xiangyu Zhang, Shaoqing Ren, and Jian Sun. Deep residual learning for image recognition. In *Proceedings of the IEEE conference on computer vision and pattern recognition*, pages 770–778, 2016. 7
- [20] Lu Hou, Zhiqi Huang, Lifeng Shang, Xin Jiang, Xiao Chen, and Qun Liu. Dynabert: Dynamic bert with adaptive width

and depth. *Advances in Neural Information Processing Systems*, 33:9782–9793, 2020. 3

- [21] Sida Huang, Hongyuan Zhang, and Xuelong Li. Enhance vision-language alignment with noise. In *Proceedings of the AAAI Conference on Artificial Intelligence*, pages 17449–17457, 2025. 9
- [22] D Jia, K Han, Y Wang, Y Tang, J Guo, C Zhang, and D Tao. Efficient vision transformers via fine-grained manifold distillation. *corr abs/2107.01378* (2021). 3
- [23] Ziheng Jiao, Hongyuan Zhang, and Xuelong Li. Cnn2gnn: How to bridge cnn with gnn. *arXiv preprint arXiv:2404.14822*, 2024. 1
- [24] Alexander Kirillov, Ross Girshick, Kaiming He, and Piotr Dollár. Panoptic feature pyramid networks. In *Proceedings of the IEEE/CVF conference on computer vision and pattern recognition*, pages 6399–6408, 2019. 6, 8
- [25] Xuelong Li. Positive-incentive noise. *IEEE Transactions on Neural Networks and Learning Systems*, 2022. 9
- [26] Xuelong Li, Han Zhang, Rong Wang, and Feiping Nie. Multiview clustering: A scalable and parameter-free bipartite graph fusion method. *IEEE transactions on pattern analysis and machine intelligence*, 44(1):330–344, 2020. 1
- [27] Yanghao Li, Chao-Yuan Wu, Haoqi Fan, Karttikeya Mangalam, Bo Xiong, Jitendra Malik, and Christoph Feichtenhofer. Mvitv2: Improved multiscale vision transformers for classification and detection. In *Proceedings of the IEEE/CVF conference on computer vision and pattern recognition*, pages 4804–4814, 2022. 2, 6
- [28] Tsung-Yi Lin, Michael Maire, Serge Belongie, James Hays, Pietro Perona, Deva Ramanan, Piotr Dollár, and C Lawrence Zitnick. Microsoft coco: Common objects in context. In *Computer Vision–ECCV 2014: 13th European Conference, Zurich, Switzerland, September 6–12, 2014, Proceedings, Part V 13*, pages 740–755. Springer, 2014. 6
- [29] Ze Liu, Yutong Lin, Yue Cao, Han Hu, Yixuan Wei, Zheng Zhang, Stephen Lin, and Baining Guo. Swin transformer: Hierarchical vision transformer using shifted windows. In *Proceedings of the IEEE/CVF international conference on computer vision*, pages 10012–10022, 2021. 1, 2, 3, 4, 6, 7
- [30] Zhenhua Liu, Yunhe Wang, Kai Han, Wei Zhang, Siwei Ma, and Wen Gao. Post-training quantization for vision transformer. *Advances in Neural Information Processing Systems*, 34:28092–28103, 2021. 4
- [31] Paul Michel, Omer Levy, and Graham Neubig. Are sixteen heads really better than one? *Advances in neural information processing systems*, 32, 2019. 3
- [32] Subhabrata Mukherjee and Ahmed Awadallah. Xtremedistil: Multi-stage distillation for massive multilingual models. *arXiv preprint arXiv:2004.05686*, 2020. 3
- [33] Xuran Pan, Tianzhu Ye, Dongchen Han, Shiji Song, and Gao Huang. Contrastive language-image pre-training with knowledge graphs. *Advances in Neural Information Processing Systems*, 35:22895–22910, 2022. 1
- [34] Xuran Pan, Tianzhu Ye, Zhuofan Xia, Shiji Song, and Gao Huang. Slide-transformer: Hierarchical vision transformer with local self-attention. In *Proceedings of the IEEE/CVF conference on computer vision and pattern recognition*, pages 2082–2091, 2023. 2, 6
- [35] Jongwoo Park, Kumara Kahatapitiya, Donghyun Kim, Shivchander Sudalairaj, Quanfu Fan, and Michael S Ryoo. Grafting vision transformers. In *Proceedings of the IEEE/CVF Winter Conference on Applications of Computer Vision*, pages 1145–1154, 2024. 7
- [36] Gabriele Prato, Ella Charlaix, and Mehdi Rezagholizadeh. Fully quantized transformer for machine translation. *arXiv preprint arXiv:1910.10485*, 2019. 4
- [37] Alec Radford, Jong Wook Kim, Chris Hallacy, Aditya Ramesh, Gabriel Goh, Sandhini Agarwal, Girish Sastry, Amanda Askell, Pamela Mishkin, Jack Clark, Gretchen Krueger, and Ilya Sutskever. Learning transferable visual models from natural language supervision. In *Proceedings of the 38th International Conference on Machine Learning, ICML 2021, 18–24 July 2021, Virtual Event*, pages 8748–8763. PMLR, 2021. 1
- [38] Ilija Radosavovic, Raj Prateek Kosaraju, Ross Girshick, Kaiming He, and Piotr Dollár. Designing network design spaces. In *Proceedings of the IEEE/CVF conference on computer vision and pattern recognition*, pages 10428–10436, 2020. 7
- [39] Joseph Redmon and Ali Farhadi. Yolov3: An incremental improvement. *arXiv preprint arXiv:1804.02767*, 2018. 2
- [40] Hongyu Ren, Hanjun Dai, Zihang Dai, Mengjiao Yang, Jure Leskovec, Dale Schuurmans, and Bo Dai. Combiner: Full attention transformer with sparse computation cost. *Advances in Neural Information Processing Systems*, 34:22470–22482, 2021. 6
- [41] Ramprasaath R Selvaraju, Michael Cogswell, Abhishek Das, Ramakrishna Vedantam, Devi Parikh, and Dhruv Batra. Grad-cam: Visual explanations from deep networks via gradient-based localization. In *Proceedings of the IEEE international conference on computer vision*, pages 618–626, 2017. 7
- [42] Kumar Shridhar, Harshil Jain, Akshat Agarwal, and Denis Kleyko. End to end binarized neural networks for text classification. In *Proceedings of SustaiNLP: Workshop on Simple and Efficient Natural Language Processing*, pages 29–34, 2020. 4
- [43] David So, Quoc Le, and Chen Liang. The evolved transformer. In *International conference on machine learning*, pages 5877–5886. PMLR, 2019. 4
- [44] Daniel A Spielman and Shang-Hua Teng. Spectral sparsification of graphs. *SIAM Journal on Computing*, 40(4):981–1025, 2011. 4
- [45] Robin Strudel, Ricardo Garcia, Ivan Laptev, and Cordelia Schmid. Segmenter: Transformer for semantic segmentation. In *Proceedings of the IEEE/CVF international conference on computer vision*, pages 7262–7272, 2021. 1
- [46] Mingxing Tan and Quoc Le. Efficientnet: Rethinking model scaling for convolutional neural networks. In *International conference on machine learning*, pages 6105–6114. PMLR, 2019. 2, 6
- [47] Mingxing Tan, Ruoming Pang, and Quoc V Le. Efficientdet: Scalable and efficient object detection. In *Proceedings of the IEEE/CVF conference on computer vision and pattern recognition*, pages 10781–10790, 2020. 6

- [48] Hugo Touvron, Matthieu Cord, Matthijs Douze, Francisco Massa, Alexandre Sablayrolles, and Hervé Jégou. Training data-efficient image transformers & distillation through attention. In *International conference on machine learning*, pages 10347–10357. PMLR, 2021. 2, 3, 6, 7
- [49] Ashish Vaswani. Attention is all you need. *arXiv preprint arXiv:1706.03762*, 2017. 1, 2
- [50] Junying Wang, Hongyuan Zhang, and Yuan Yuan. Adv-cpg: A customized portrait generation framework with facial adversarial attacks. In *Proceedings of the IEEE/CVF Conference on Computer Vision and Pattern Recognition*, 2025. 1
- [51] Ningning Wang, Guobing Gan, Peng Zhang, Shuai Zhang, Junqiu Wei, Qun Liu, and Xin Jiang. Clusterformer: Neural clustering attention for efficient and effective transformer. In *Proceedings of the 60th Annual Meeting of the Association for Computational Linguistics (Volume 1: Long Papers)*, pages 2390–2402, 2022. 6
- [52] Wenhai Wang, Enze Xie, Xiang Li, Deng-Ping Fan, Kaitao Song, Ding Liang, Tong Lu, Ping Luo, and Ling Shao. Pyramid vision transformer: A versatile backbone for dense prediction without convolutions. In *Proceedings of the IEEE/CVF international conference on computer vision*, pages 568–578, 2021. 2, 4, 6, 7
- [53] Ziheng Wang, Jeremy Wohlwend, and Tao Lei. Structured pruning of large language models. *arXiv preprint arXiv:1910.04732*, 2019. 3
- [54] Cong Wei, Brendan Duke, Ruowei Jiang, Parham Aarabi, Graham W Taylor, and Florian Shkurti. Sparsifiner: Learning sparse instance-dependent attention for efficient vision transformers. In *Proceedings of the IEEE/CVF Conference on Computer Vision and Pattern Recognition*, pages 22680–22689, 2023. 6
- [55] Bichen Wu, Chaojian Li, Hang Zhang, Xiaoliang Dai, Peizhao Zhang, Matthew Yu, Jialiang Wang, Yingyan Lin, and Peter Vajda. Fbnetv5: Neural architecture search for multiple tasks in one run. *arXiv preprint arXiv:2111.10007*, 2021. 6
- [56] Zhuofan Xia, Xuran Pan, Shiji Song, Li Erran Li, and Gao Huang. Vision transformer with deformable attention. In *Proceedings of the IEEE/CVF conference on computer vision and pattern recognition*, pages 4794–4803, 2022. 7
- [57] Tete Xiao, Yingcheng Liu, Bolei Zhou, Yuning Jiang, and Jian Sun. Unified perceptual parsing for scene understanding. In *Proceedings of the European conference on computer vision (ECCV)*, pages 418–434, 2018. 6, 8
- [58] Yunyang Xiong, Hanxiao Liu, Suyog Gupta, Berkin Akin, Gabriel Bender, Yongzhe Wang, Pieter-Jan Kindermans, Mingxing Tan, Vikas Singh, and Bo Chen. Mobiledeets: Searching for object detection architectures for mobile accelerators. In *Proceedings of the IEEE/CVF conference on computer vision and pattern recognition*, pages 3825–3834, 2021. 6
- [59] Yanchen Xu, Siqi Huang, Hongyuan Zhang, and Xuelong Li. Why does dropping edges usually outperform adding edges in graph contrastive learning? In *Proceedings of the AAAI Conference on Artificial Intelligence*, pages 21824–21832, 2025. 9
- [60] Jianwei Yang, Chunyuan Li, Pengchuan Zhang, Xiyang Dai, Bin Xiao, Lu Yuan, and Jianfeng Gao. Focal self-attention for local-global interactions in vision transformers. *arXiv preprint arXiv:2107.00641*, 2021. 7
- [61] Haoran You, Yunyang Xiong, Xiaoliang Dai, Bichen Wu, Peizhao Zhang, Haoqi Fan, Peter Vajda, and Yingyan Celine Lin. Castling-vit: Compressing self-attention via switching towards linear-angular attention at vision transformer inference. In *Proceedings of the IEEE/CVF Conference on Computer Vision and Pattern Recognition*, pages 14431–14442, 2023. 2, 4, 6
- [62] G Yu, Q Chang, W Lv, C Xu, C Cui, W Ji, Q Dang, K Deng, G Wang, Y Du, et al. Pp-picodet: A better real-time object detector on mobile devices. arxiv 2021. *arXiv preprint arXiv:2111.00902*. 6, 7
- [63] Manzil Zaheer, Guru Guruganesh, Kumar Avinava Dubey, Joshua Ainslie, Chris Albeti, Santiago Ontanon, Philip Pham, Anirudh Ravula, Qifan Wang, Li Yang, et al. Big bird: Transformers for longer sequences. *Advances in neural information processing systems*, 33:17283–17297, 2020. 4
- [64] Hongyuan Zhang, Jiankun Shi, Rui Zhang, and Xuelong Li. Non-graph data clustering via $\mathcal{O}(n)o(n)$ bipartite graph convolution. *IEEE Transactions on Pattern Analysis and Machine Intelligence*, 45(7):8729–8742, 2023. 2, 4
- [65] Hongyuan Zhang, Sida Huang, Yubin Guo, and Xuelong Li. Variational positive-incentive noise: How noise benefits models. *IEEE Transactions on Pattern Analysis and Machine Intelligence*, 2024. 9
- [66] Hongyuan Zhang, Yanchen Xu, Sida Huang, and Xuelong Li. Data augmentation of contrastive learning is estimating positive-incentive noise. *arXiv preprint arXiv:2408.09929*, 2024. 9
- [67] Hongyuan Zhang, Yanan Zhu, and Xuelong Li. Decouple graph neural networks: Train multiple simple gnns simultaneously instead of one. *IEEE Transactions on Pattern Analysis and Machine Intelligence*, 2024. 2
- [68] Bolei Zhou, Hang Zhao, Xavier Puig, Sanja Fidler, Adela Barriuso, and Antonio Torralba. Scene parsing through ade20k dataset. In *Proceedings of the IEEE conference on computer vision and pattern recognition*, pages 633–641, 2017. 6
- [69] Daquan Zhou, Bingyi Kang, Xiaojie Jin, Linjie Yang, Xiaochen Lian, Zihang Jiang, Qibin Hou, and Jiashi Feng. Deepvit: Towards deeper vision transformer. *arXiv preprint arXiv:2103.11886*, 2021. 3
- [70] Lei Zhu, Xinjiang Wang, Zhanghan Ke, Wayne Zhang, and Rynson WH Lau. Biformer: Vision transformer with bi-level routing attention. In *Proceedings of the IEEE/CVF conference on computer vision and pattern recognition*, pages 10323–10333, 2023. 2, 6